Investigation of Mechanisms Underlying Takotsubo Syndrome Using an Electromechanical Heart Model

Carola Kruthoff[1], Jonathan Krauß[1], Aylin Seedorf[2], Katrin Streckfuß-Bömeke[2,3], Tim Meyer[2], Axel Loewe[1]

[1] Institute of Biomedical Engineering, Karlsruhe Institute of Technology (KIT), Karlsruhe, Germany,
[2] University Medical Centre Göttingen, Göttingen, Germany,
[3] Julius-Maximilians-University Würzburg, Würzburg, Germany

Abstract

Takotsubo syndrome (TTS) is a reversible form of heart failure characterized by a transient ballooning of the left ventricle (LV) and a rightward shift of the pressure-volume-loop (pV loop). The underlying pathophysiology of TTS remains unclear, with hypotheses ranging from a corruption of Purkinje-muscle junctions (PMJs) to changes in active stress development (T_a).

We divided the ventricles into an apical and a basal region for four simulations (A-D). For scenario A, we deactivated all PMJs in the apical region. We modeled the absence of T_a in the apical region (B) and doubled T_a in the basal region (C). For D, we combined B and C. All results were compared to an unaltered control simulation.

Deactivation of the PMJs showed no change in LV ejection fraction (LVEF) and could not reproduce apical ballooning. Both scenarios B and D led to visible ballooning, a lower LVEF (B: 37.45%, D: 43.91%) than in the control scenario (56.59%) and a rightward shift of the pV loop. Scenario C, showed a slightly stronger basal constriction and minimal change in LVEF compared to the control.

Our findings suggest that corruption of apical PMJs cannot be the sole cause for the TTS phenotype. Hypo-contractility in the apex appears to be the main factor driving apical ballooning, while basal hyper-contractility could be an amplifying mechanism.

1. Introduction

Takotsubo Syndrome (TTS) refers to a reversible form of heart failure leading to regional ventricular contraction irregularities. It typically affects postmenopausal women following a stressful trigger. Out of all women presenting at clinics with acute coronary syndrome, up to $20\,\%$ are diagnosed with TTS [1]. The most common TTS phenotype - called apical type - is observed in $> 80\,\%$ of TTS patients [2]. The apical type is characterized by a transient ballooning of the left ventricle combined with basal hyper-contractility during systole (Figure 1). This ballooning is typically accompanied by a rightward shift of the pressure-volume-loop (pV loop) [3].

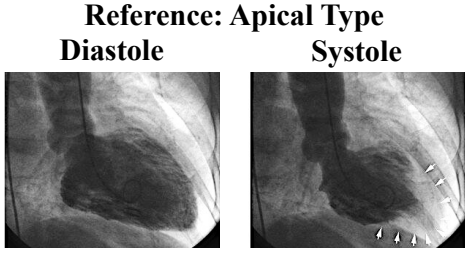

Figure 1. Angiograms of the LV with apical phenotype. Adapted from [4] under the CC BY 2.0 license.

The pathophysiology underlying TTS remains largely unclear. TTS patients have shown increased sympathetic nerve activity as well as elevated levels of norepinephrine, pointing to an enhanced release of myocardial catecholamines. However, the exact mechanism connecting these effects to the ballooning remain elusive [1]. The combination of hypo-contractility in the apex and hyper-contractility close to the base could also suggest a delayed activation in the apex due to impaired Purkinje-muscle junctions (PMJs) in this region. In this work, we use an electromechanical heart model to verify which basic mechanisms reproduce the apical TTS phenotype.

2. Methods

2.1. Study Setup

We hypothesized that four different scenarios (A-D) could reproduce apical ballooning:

• **Scen. A:** Deactivation of all PMJs in the apical region. Conduction and active stress development (T_a) in the myocardium stayed intact.

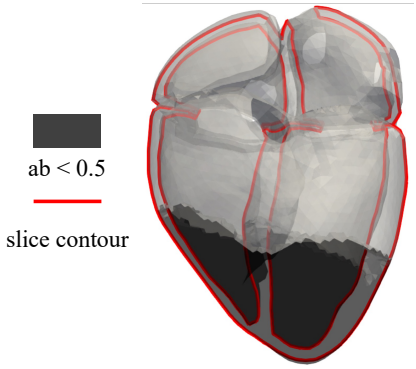

Figure 2. Visualization of apical and basal region based on the ab-coordinate and the position of the 4-chamber-slice.

- **Scen. B:** Deactivation of T_a in the apical region.
- **Scen. C:** Doubling of T_a in the basal region.
- **Scen. D:** Deactivation of T_a in the apical region and doubling of T_a in the basal region (B+C).

All results were compared to a control simulation without any alterations. We used the apico-basal coordinate (ab) of the consistent biventricular coordinate system [5] to divide the ventricles into an apical (ab < 0.5) and a basal region (ab ≥ 0.5) (Figure 2).

For analysis, we visualized the systolic shape of the heart with a 4-chamber slice (Figure 2). The left ventricular ejection fraction (LVEF) was calculated to quantify the impact on cardiac output. Stiermaier et al. [3] identified a rightward shift of the *pV* loop as a clear characteristic of TTS. Therefore, we compared the *pV* loops for control and altered simulations.

2.2. Simulation Framework

We used two different simulation frameworks, a uni-directionally coupled framework for scenario A and a fully coupled one for scenario B-D. All simulations were performed with the same whole heart mesh derived from MRI data of a 33-year old healthy volunteer [6]. The electrophysiology mesh had a mean edge length of $0.8\,\mathrm{mm}$. The mechanical simulation used a lower resolution version of the electrophysiology mesh, which also incorporated vessel trunks and a pericardium. The mean edge length of the whole mechanics mesh was $3.17\,\mathrm{mm}$. The ionic models used for all simulations are listed in Table 1. In both frameworks, hemodynamics were simulated with a 0D closed-looped model coupled to the mechanical system to guarantee volume consistency between the 3D mechanical and 0D hemodynamical models [7].

The basic cycle length was set to $48\,\mathrm{bpm}$.

Table 1. Overview of used ionic models.

	Scenario A	**Scenario B-D**
Atria	Courtemanche [8]	
Ventricles	Tomek [9]	OHaraRudy [10]
HPS	Stewart [11]	-

Only scenario A incorporated a His-Purkinje system (HPS), which was generated as a fractal tree, using anatomical landmarks and sites of earliest activation for guidance [12]. The tree is linked to the myocardium via Purkinje Muscle Junctions (PMJs), where each end of the network is connected to 15 nodes in the myocardium via a resistive element. The electrophysiology simulations for scenario A and its control were performed with openCARP [13]. The monodomain conductivities for ventricular regions were adopted from [14] and for atrial regions from [15]. We obtained transmembrane voltages ($\mathrm{V_m}$) as a result of monodomain simulations. The local activation time (LAT) of each node was defined as the time, when $\mathrm{V_m}$ crossed a threshold of $-50\,\mathrm{mV}$ with a positive slope. The mechanics simulations were done with CardioMechanics [16] and used the LATs from the third heart cycle as input for the tension model by Niederer et al. [17]. Due to noticeable drifting in the first three *pV* loops, we simulated mechanics for five cycles and analyzed only the last one.

Scenarios B-D were simulated using CardioMechanics in a fully coupled configuration, including the effects of calcium binding to troponin and mechano-electrical feedback [15]. The electrophysiology simulations were also based on the monodomain model with conductivities chosen according to [15]. For the mechanics simulation, we used the tension model by Land et al. [18] and evaluated the results from the fifth heart cycle.

The HPS in scenario A could only be modeled in openCARP, which does not facilitate mechanical simulations. Hence, the uni-directional coupling enabled an electromechanical simulation incorporating an explicit model of the HPS and its PMJs. The fully coupled framework is deemed to be more exact and was used for the scenarios in which no explicit HPS model was required. For this setup a HPS was imitated by stimulating in the ventricles at three typical points of early activation.

3. Results

Figure 3 shows the systolic shape outline of all four simulations compared to their control (gray) with the blood pool in the left ventricle (LV) highlighted as a shaded area. Scenario A does not show a difference in systolic shape compared to the control; the only observed difference was a slight delay in the onset of contraction. Scenario B ex-

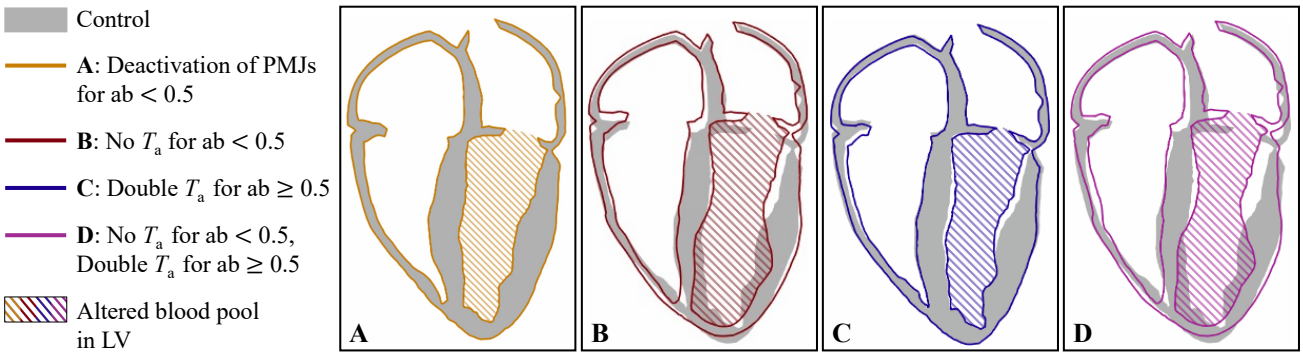

Figure 3. 4-chamber slice of all simulations at systole. The healthy control simulation is shown as a gray surface, while the outline of the altered scenario is depicted in color. The bloop pool in the LV is shaded.

hibited a visible ballooning effect, which was even more pronounced in scenario D. The systolic shape of scenario C showed a slightly stronger constriction in the basal area compared to the control, but did not resemble the TTS phenotype.

The LVEF of all simulations is summarized in Table 2. The deactivation of the PMJs had no effect on the LVEF and the LV pV loop. The explicit model of the HPS resulted in a higher LVEF than in the fully coupled scenario. Scenario B and D demonstrated a severe reduction in LVEF (B: 36.1 %, C: 43.4 %) compared to their control (56.6 %). Both scenarios also showed a rightward shift of the LV pV loop compared to control (Figure 4). Scenario D exhibited a partial recovery of pump function compared to scenario B, which can also be seen in the pV loop of scenario D being in between the pV loop of the control on the left and scenario B on the right. The doubling of T_a in scenario C led to a slight increase in LVEF. The LV pV loop of C was shifted to the left and also demonstrated a visible increase in size compared to its control.

Table 2. LVEF of all scenarios and their control.

Description	Scen.	LVEF (%)
Control (Unidirectional Coupling)		65.4
Deactivation of PMJs for ab < 0.5	A	65.4
Control (Fully Coupled)		56.6
No T_a for ab < 0.5	B	36.1
Double T_a for ab ≥ 0.5	C	59.7
No T_a for ab < 0.5, Double T_a for ab ≥ 0.5	D	43.4

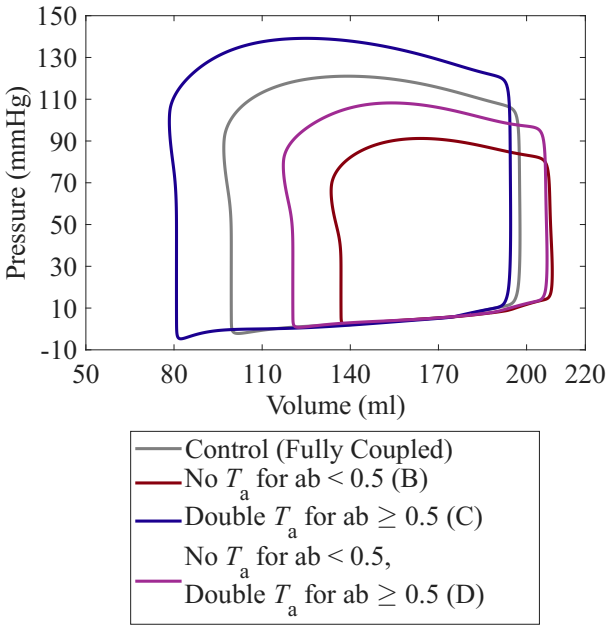

Figure 4. Comparison of LV pV loops for all simulations with varying T_a and their control.

4. Discussion

The deactivation of the PMJs in the apex has virtually no acute effect on hemodynamics and the systolic shape of the ventricles. The delayed activation in the apex is mostly visible in the LATs and in a slight delay of apical contraction onset. Considering these results, impaired PMJs in the apex cannot be the sole cause for the TTS phenotype. The higher LVEF, compared to the fully coupled simulation, may be due to the activation from an explicit HPS being more effective than the activation from three points.

Both the systolic shape and hemodynamic changes in scenarios B and D suggest that a severe reduction of T_a in the apex is the primary mechanism responsible for apical ballooning. An increase in T_a close to the base as applied in scenario C and D could be an amplifying mechanism. The basal hyper-contractility in addition to hypo-contractility in the apex leads to a partial recovery in pump

function. This recovery effect suggests that the hypercontractility could be a compensatory mechanism following the apical stunning and major decrease in LVEF.

Comparing the relative decrease in LVEF due to the alterations in our simulations (B: $-35\,\%$, C: $-23\,\%$) to the $-23\,\%$ decrease for TTS patients in clinical data [3], suggests that a combination of apical hypo- and basal hypercontractility can best reproduce the TTS phenotype. A visual comparison of the LV *pV* loops of scenario B and D to the LV *pV* loops in [3] show a similar increase in end-diastolic and end-systolic volumes. The LV stroke volume of TTS patients in [3] was mostly preserved and the systolic pressure was almost the same for TTS patients and the control group. Our simulations demonstrate a noticeable decrease in LV stroke volume and systolic pressure. These differences imply that further mechanisms contribute to the TTS phenotype, which are not yet captured in this model.

5. Conclusion

Our findings show that an impairment of apical PMJs alone does not cause apical ballooning. Instead, they suggest apical hypo-contractility to be a leading mechanism in the forming of apical ballooning. A combination of apical hypo- and basal hyper-contractility best reproduces the TTS phenotype regarding systolic shape and hemodynamic properties. The exact relationship between the visible hypo- and hyper-contractility and the measured sympathetic overdrive [1] warrants further investigation in future work.

Acknowledgments

This work was supported by the Deutsche Forschungsgemeinschaft (DFG, German Research Foundation) – Project numbers 465189069, 507828355 and by the Federal Ministry of Research, Technology and Space under the grant number 13GW0724D. This work was performed on the computational resource bwUniCluster funded by the Ministry of Science, Research and the Arts and the universities of Baden-Württemberg, within the framework program bwHPC.

References

[1] Rawish E, et al. Current Knowledge and Future Challenges in Takotsubo Syndrome. J Clin Med Jan. 2021;10(3):479.

[2] Templin C, et al. Clinical Features and Outcomes of Takotsubo (Stress) Cardiomyopathy. N Engl J Med Sep. 2015; 373(10):929–938.

[3] Stiermaier T, et al. Hemodynamic Assessment in Takotsubo Syndrome. J Am Coll Cardiol May 2023;81(20):1979–1991.

[4] Patankar G, et al. Reverse Takotsubo Cardiomyopathy: Two Case Reports and Review of the Literature. J Med Case Reports 2013;7(1):84.

[5] Schuler S, et al. Cobiveco: Consistent Biventricular Coordinates for Precise and Intuitive Description of Position in the Heart – with MATLAB Implementation. Med Image Anal Dec. 2021;74:102247.

[6] Gerach T, et al. Four-Chamber Human Heart Model for the Simulation of Cardiac Electrophysiology and Cardiac Mechanics, Oct. 2021. URL `https://zenodo.org/records/5573921`.

[7] Gerach T, et al. Electro-Mechanical Whole-Heart Digital Twins: A Fully Coupled Multi-Physics Approach. Mathematics May 2021;9(11):1247.

[8] Courtemanche M, et al. Ionic Mechanisms Underlying Human Atrial Action Potential Properties. Am J of Physiol Jul. 1998;275(1):H301–321.

[9] Tomek J, et al. Development, Calibration, and Validation of a Novel Human Ventricular Myocyte Model in Health, Disease, and Drug Block. eLife Dec. 2019;8:e48890.

[10] O'Hara T, et al. Simulation of the Undiseased Human Cardiac Ventricular Action Potential. PLOS Comput Biol May 2011;7(5):e1002061.

[11] Stewart P, et al. Mathematical Models of the Electrical Action Potential of Purkinje Fibre Cells. Philos Trans A Math Phys Eng Sci Jun. 2009;367(1896):2225–2255.

[12] Correas M, et al. Automated Generation of Purkinje Networks in the Human Heart Considering the Anatomical Variability. In Functional Imaging and Modeling of the Heart, volume 13958. Springer Nature Switzerland, Jun. 2023; 127–136.

[13] Plank G, et al. The openCARP Simulation Environment for Cardiac Electrophysiology. Comput Methods Programs Biomed Sep. 2021;208:106223.

[14] Kruthoff C, et al. Evaluating the Effects of Left Bundle Branch Block in an Electromechanical Heart Model. Curr Dir Biomed Eng Sep. 2025;11(1):389–392.

[15] Gerach T, et al. Differential Effects of Mechano-electric Feedback Mechanisms on Whole-heart Activation, Repolarization, and Tension. J Physiol Jan. 2024;602(18):4605–4624.

[16] Gerach T, et al. CardioMechanics, Sep. 2023. URL `https://github.com/KIT-IBT/CardioMechanics/tree/main`.

[17] Niederer S, et al. Length-Dependent Tension in the Failing Heart and the Efficacy of Cardiac Resynchronization Therapy. Cardiovas Res Feb. 2011;89(2):336–343.

[18] Land S, et al. A Model of Cardiac Contraction Based on Novel Measurements of Tension Development in Human Cardiomyocytes. J Mol Cell Cardiol May 2017;106:68–83.

Address for correspondence:

Karlsruhe Institute of Technology
Institute of Biomedical Engineering
Carola Kruthoff, publications@ibt.kit.edu
Fritz-Haber-Weg 1, 76131 Karlsruhe, Germany